NUREG/CR-4460
SAND85-2196
RG
Printed January 1986

Uncertainty and Sensitivity Analysis of an Upper Plenum Test Problem for the MAEROS Aerosol Model

J. C. Helton, R. L. Iman, J. D. Johnson, C. D. Leigh

Prepared by
Sandia National Laboratories
Albuquerque, New Mexico 87185 and Livermore, California 94550
for the United States Department of Energy
under Contract DE-AC04-76DP00789

Prepared for
U. S. NUCLEAR REGULATORY COMMISSION

Available from

Superintendent of Documents
U.S. Government Printing Office
Post Office Box 37082
Washington, D.C. 20013-7982

and

National Technical Information Service
Springfield, VA 22161

NUREG/CR-4460
SAND85-2196
RG

UNCERTAINTY AND SENSITIVITY ANALYSIS OF AN UPPER PLENUM TEST PROBLEM FOR THE MAEROS AEROSOL MODEL

J. C. Helton,[1] R. L. Iman,[2] J. D. Johnson,[3] C. D. Leigh[2]

Printed: January, 1986

Sandia National Laboratories
Albuquerque, NM 87185
Operated by
Sandia Corporation
for the
U.S. Department of Energy

Prepared for
Division of Risk Analysis and Operations
Office of Nuclear Regulatory Research
U.S. Nuclear Regulatory Commission
Washington, DC 20555
Under Memorandum of Understanding DOE 40-550-75
NRC Fin No. A-1339

---

1 Department of Mathematics
Arizona State University
Tempe, AZ 85287

2 Safety and Environmental Studies Division
Sandia National Laboratories
Albuquerque, NM 87185

3 Science Applications International Corp.
Albuquerque, NM 87102

ABSTRACT

The MAEROS aerosol model is being incorporated into the MELCOR code system for the calculation of risk from severe reactor accidents. To gain insight to assist in this incorporation, a computational test problem involving a three component aerosol in the upper plenum of a pressurized water reactor was analyzed with MAEROS. The following topics were investigated (1) the CRAY-1 CPU time requirements to implement and solve the system of differential equations on which MAEROS is based, (2) the effects on computational time and representational accuracy due to the use of different overall section boundaries and numbers of sections and components, and (3) the behavior of the aerosol and the variables which influence this behavior. Uncertainty and sensitivity analysis techniques based on Latin hypercube sampling and regression analysis were used in the investigation. Five sections and overall section boundaries from 0.1E-6 m to 50.E-6 m were found to be adequate for the problem under consideration. Further, solution time was found to be at least several hundred times faster than real time, which is felt to be adequate for MELCOR. Stepwise regression was used to investigate the sources of variation in computational time and suspended aerosol concentration.

TABLE OF CONTENTS

LIST OF FIGURES

LIST OF FIGURES

LIST OF TABLES

ACKNOWLEDGMENT

The authors wish to acknowledge the support provided by J. L. Sprung and S. W. Webb of Sandia National Laboratories in the development of this analysis.

1. Introduction. A computational test problem for the MAEROS aerosol model (1, 2) involving a three-component aerosol in the upper plenum of a pressurized water reactor is presented. This model is being incorporated into the MELCOR risk code system (3) under development at Sandia National Laboratories. The purpose of this analysis is to gain insights with respect to (1) the CRAY-1 CPU time requirements to implement and solve the system of differential equations on which MAEROS is based, (2) the effects on computational time and representational accuracy due to the use of different overall section boundaries (i.e., minimum and maximum particle sizes), numbers of sections (i.e., particle size classes), and numbers of components (i.e., chemical species making up the aerosol), and (3) the behavior of the aerosol and the variables which influence this behavior. These insights will help in the development and ultimate application of the MELCOR code system. Further, due to the extensive interest in MAEROS and other aerosol models outside of the MELCOR effort, the presented results should be of use elsewhere. For example, MAEROS is also the aerosol model incorporated into the CONTAIN computer program (4) for severe nuclear reactor accident containment analysis.

The MAEROS aerosol model can be used to represent an aerosol in which each particle is composed of a number of different materials. In the terminology used with MAEROS, each material is referred to as a component. In the derivation of the equations for the model, the particle size range is discretized between specified minimum and maximum particle sizes into a finite number of particle size classes. Each size class is referred to as a section. Mathematically, the MAEROS aerosol model is a system of nonlinear differential equations of the form

$$dQ_{\ell k}(t)/dt = f_{\ell k}[Q(t), t], \quad \ell = 1,\ldots,m, \quad k = 1,\ldots,n, \tag{1}$$

where $Q_{\ell k}(t)$ is the concentration (kg/m^3) of component k in section ℓ at time t (sec), $Q(t)$ is the vector of all $Q_{\ell k}(t)$, m is the number of sections, and n is the number of components. The exact form of the preceding system considered in this study is given in Section 3 of Helton et al. (5).

The number of equations in the system in (1) is equal to the product of the number of sections and the number of components (i.e., mn). Thus, reducing the number of sections or components for a given problem will reduce the size of the system of differential equations and may significantly reduce the computational costs associated with solving the system. Further, appropriate selection of overall section boundaries may reduce computational costs by making efficient use of the number of sections selected. For example, due to rapid agglomeration, inclusion of very small particle sizes can greatly increase computational costs but have no effect on aerosol properties of interest (e.g., aerosol mass concentration or mass median diameter).

This presentation is organized as follows. The aerosol problem under consideration is described in Section 2. Then, the effects due to section boundaries, number of sections, and number of components are considered in Sections 3, 4 and 5, respectively. A sensitivity analysis for computational time requirements and

suspended concentration of individual aerosol components is presented in Section 6. Finally, a summary discussion is given in Section 7.

2. Problem for Analysis. As already indicated, this presentation involves a three-component aerosol in the upper plenum of a pressurized water reactor. The reactor is assumed to be undergoing a severe accident with uncovering of and damage to the fuel rods. The three aerosol components are assumed to be CsI, CsOH, and other materials, respectively. The variables considered in the analysis are listed in Table I. The upper plenum is assumed to have a volume of 15.5 m^3; the particle slip coefficient, which is used in the calculation of size-dependent slip correction factors, is taken to be 1.37, and no water condensation is assumed.

To determine computational time requirements and other system properties, a set of 50 MAEROS runs was made for each of various formulations of the system of equations indicated in (1). The variable values used as input to MAEROS were obtained by generating a Latin hypercube sample (6, 7) of size 50 for the variables in Table I. The restricted pairing technique of Iman and Conover (8) was used in generating the sample to induce the desired correlation structure (see Table I). Further, the inequality involving x and γ was implemented as described in Equation (5.2) of Helton et al. (5). Various graphical techniques and stepwise regression were used to examine input-output relationships as a means of understanding the behavior of the system.

3. Effects Due to Section Boundaries. The problem was first analyzed with 10 sections and overall section boundaries of 0.01E-6 m to 50.E-6 m, 0.1E-6 m to 50.E-6 m, and 0.1E-6 m to 100.E-6 m, respectively. The effect of these boundaries on the computational time required to evaluate one set of coefficients (i.e., the β's and ρ's in Tables 3.1, 3.2 and 3.3 of Helton et al. (5)) for the system of differential equations representing aerosol behavior is shown in Figure 1. This figure contains three estimated cumulative distribution functions. Each of these estimated distribution functions corresponds to one set of section boundaries and was constructed from the results of 50 MAEROS runs performed for the previously indicated Latin hypercube sample. Such distribution functions are used in several places in this presentation to display observed variability in model behavior. As can be seen from Figure 1, approximately 0.57 sec to 0.71 sec of CPU time was required to evaluate the coefficients for section boundaries of 0.1E-6 m to 50.E-6 m (curve 2), while boundaries of 0.1E-6 m to 100.E-6 m (curve 3) and 0.01E-6 m to 50.E-6 m (curve 1) required approximately 10% and 20% more time, respectively.

For 3 components and 10 sections, a system of 30 differential equations results for each pair of section boundaries and each element of the Latin hypercube sample. These systems were solved with the Runge-Kutta differential equation solver RKF45 (9), which is incorporated into MAEROS. Relative and absolute error tolerances of 10^{-3} and 10^{-20}, respectively, were used. For section boundaries of 0.1E-6 m to 50.E-6 m, Figure 2 shows the distribution of time required to solve the resultant systems of equations for time intervals of 1, 5, 10 and 30 seconds. Further, Figure 3 shows distributions for the ratio of problem time to solution time (i.e., t_p/t_s, where t_p is the time period (sec) over which aerosol behavior is considered and t_s is the CPU time (sec) required to solve the system in (1) from $t=0$ to $t=t_p$). This ratio varied from approximately 25 to 400, with the smaller

ratios associated with the shorter time intervals. As indicated in Figure 4, the solutions approach an asymptote at or before about 30 sec. In this problem, no aerosol movement out of the upper plenum is assumed. Such movement could affect aerosol behavior and the form of the asymptote. However, in the implementation of MELCOR, the movement of aerosols out of control volumes will take place between system time steps rather than continuously during such steps; hence, the present approach is consistent with MELCOR implementation.

The solution times for section boundaries of 0.01E-6 m to 50.E-6 m were much greater than for boundaries of 0.1E-6 m to 50.E-6 m, while the solution times for section boundaries of 0.1E-6 m to 100.E-6 m were quite similar to those for boundaries of 0.1E-6 m to 50.E-6 m. Figure 5 illustrates this behavior for solutions from 0 sec to 30 sec. The following notation is used in conjunction with this figure:

X_1 ~ solution (CPU) time, 0.1E-6 m to 50. E-6 m
Y_1 ~ solution (CPU) time, 0.1E-6 m to 100.E-6 m
Y_2 ~ solution (CPU) time, 0.01E-6 m to 50.E-6 m
$X \sim (X_1, Y_1)$, $0 \sim (X_1, Y_2)$.

The variable X_1 is represented on the abscissa of Figure 5, while Y_1 and Y_2 are represented on the ordinate. Fifty values of $X \sim (X_1, Y_1)$ and $0 \sim (X_1, Y_2)$ appear in the figure (i.e., one for each of the 50 Latin hypercube sample vectors). The straight line labeled (X_1, X_1) in Figure 5 passes through the origin and has slope 1. If the solution times associated with a given sample vector but different overall section boundaries are the same, then the corresponding points X and 0 will fall on this line. In contrast, the appearance of a point above this line indicates that more solution time was required than with boundaries of 0.1E-6 m to 50.E-6 m, and the appearance of a point below this line indicates that less solution time was required. Thus, Figure 5 shows that, for solutions from 0 sec to 30 sec, solution times for overall section boundaries of 0.1E-6 m to 50.E-6 m (i.e., X_1) and 0.1E-6 m and 100.E-6 m (i.e., Y_1) are essentially identical, while solution times for boundaries of 0.01E-6 m to 50.E-6 m (i.e., Y_2) are higher by factors of approximately 5 to 20. Such plots will be used several times in this presentation to display variability in model behavior.

If the different section boundaries produce similar solutions, the boundaries of 0.1E-6 m to 50.E-6 m would be preferable on a computational basis. The solutions cannot be compared on a section by section basis because the section boundaries are not the same when different lower and upper section boundaries are used. However, the total suspended mass can be compared. This comparison was made and the choice of section boundaries was found to have essentially no effect on total suspended mass. Figure 6 illustrates this comparison. Thus, section boundaries of 0.1E-6 m to 50.E-6 m appear to be adequate for this problem.

In some cases, the assumed distributions for geometric standard deviation (i.e., GSD1, GSD2 and GSD3) and mass median diameter (i.e., MMD1, MMD2 and MMD3) result in a significant fraction of the entering component mass being in particles

smaller than the particles contained in the lowest section. In such cases, particle mass was distributed over the sections actually considered. Specifically, the geometric expected value (calculated from the assumed mass median diameter) and the geometric standard deviation of the entering particles were used to calculate the shape of the particle mass distribution. Then, the assumed total mass of the entering particles was apportioned according to this distribution between the lower and upper section boundaries. The fact that no difference in total suspended mass was encountered when this apportioning scheme was used with boundaries of 0.01E-6 m to 50.E-6 m and 0.1E-6 m to 50.E-6 m further indicates the limited importance of particles between 0.01E-6 m and 0.1E-6 m for the problem under consideration. Another apportioning scheme would be to calculate the mass of particles below the lowest section boundary and then to enter this mass into the lowest section under consideration. However, as no difference in total suspended mass was observed with lower boundaries of 0.01E-6 m and 0.1E-6 m, the question of which apportioning scheme to use seems to be rather unimportant.

4. Effects Due to Number of Sections. As already discussed, section boundaries of 0.1E-6 m to 50.E-6 m appear to be adequate for this problem. The effects due to the number of sections used between these boundaries is now investigated. Specifically, analyses were performed using 5, 10 and 15 sections. The effect of the number of sections on the computational time required to evaluate one set of coefficients for the system of differential equations representing aerosol behavior is shown in Figure 7. The distributions appearing in this figure are based on 50 coefficient evaluations for each case using the previously described Latin hypercube sample. The coefficient evaluations for 5 sections required approximately 0.3 sec of CPU time, while the evaluations for 10 and 15 sections required about 2 and 4 times as much time, respectively.

As this problem is for 3 components, systems of 15, 30 and 45 differential equations result for 5, 10 and 15 sections, respectively. As before, these systems were solved with the Runge-Kutta differential equation solver RKF45. Relative and absolute error tolerances of 10^{-3} and 10^{-20}, respectively, were used. The distributions of solution times associated with the previously considered coefficients are shown in Figures 8, 2 and 9 for 5, 10 and 15 sections, respectively. As examination of these figures shows, the solutions for 15 sections required approximately 10 times as much CPU time as the solutions for 5 sections while the solutions for 10 sections required approximately 4 times as much CPU time as the solutions for 5 sections. This comparison is shown more explicitly in Figure 10 for solutions from 0 sec to 30 sec.

If solutions for 5, 10 and 15 sections are similar, then use of 5 sections is computationally more efficient than use of a larger number of sections. The solutions for total suspended mass were compared for 5, 10 and 15 sections and found to be very similar. Such a comparison is shown in Figure 11. For this problem, it appears that the use of 5 sections is adequate. Figure 12 shows the ratio of problem time to solution time for 5 sections; Figure 3 contains the same information for 10 sections. As shown in these figures, the ratio of problem time to solution time varies between 25 and 400 for 10 sections and between 100 and 1100 for 5 sections.

5. Effects Due to Number of Components. The number of equations in the MAEROS system increases linearly with the number of components under consideration. A possible way to reduce computational time is to solve a system of differential equations in which all particle mass is assumed to be concentrated in a single component and then to solve a system of algebraic equations at the end of each solution time step to approximate the mass associated with each component in each section (10). To provide an indication of the amount of computational time that might be saved by such a procedure, the systems for 10 sections and boundaries of 0.1E-6 m to 50.E-6 m were reformulated and solved with the mass in each section concentrated in a single component. This reduces each system from 30 equations to 10 equations. Although reducing the number of components from 3 to 1 reduced the required computational time, the effect was not large. As shown in Figure 13 for solution time from 0 sec to 30 sec, reducing the number of components reduced the solution time by about 30%. In contrast, variation of the variables in Table I caused solution time from 0 sec to 30 sec to vary by a factor of 4, and reduction of the number of sections from 15 to 5 reduced solution time by a factor of 10.

6. Sensitivity Analysis. After the MAEROS calculations were completed, a sensitivity analysis was performed to determine which of the variables in Table I are most important in influencing the time required to evaluate the required coefficients and solve the associated system of equations and also in influencing the suspended concentrations of the three components. This determination was made on the basis of stepwise regression using a program available at Sandia National Laboratories (11). Regressions were performed on both raw and rank-transformed data for the case involving 5 sections and section boundaries of 0.1E-6 m to 50.E-6 m. The designation "raw data" denotes the input and output variables as originally used or generated in the analysis. The designation "rank-tranformed data" denotes the variables after they have been transformed by giving the smallest value of each variable the value of 1, the next largest value of each variable the value of 2, and so on up to the largest value of each variable which is given the value of 50, where 50 is the size of the sample being analyzed. The rank transform often facilitates regression analyses when outliers or nonlinear relationships between independent and dependent variables are present (12).

The results of the regression analyses are presented in Tables II through VI. A variable was required to be significant at the 0.02 α-level to enter a regression model and to remain significant at the 0.05 α-level to stay in the regression model once entered. The behavior of R^2 values and PRESS (PRedicted Error Sum of Squares) values were also considered in selecting the stopping points for the stepwise regressions presented in the indicated tables. The PRESS value is used to assure that the selected regression model is not overfitting the data on which it is based (13). Additional background on the approach to sensitivity analysis being used is available elsewhere (5, 14, 15, 16).

The regression analyses for the CPU time required to evaluate the MAEROS coefficients are given in Table II. The distribution of CPU time under consideration is shown in Figure 7 (curve 1). The variability in CPU time is dominated by χ (dynamic shape factor) and ϵ (turbulence dissipation rate). However, as indicated in Figure 7, the variability in this time is not large.

The regression analyses for the CPU time required to solve the MAEROS equations are given in Table III. The distribution of CPU time under consideration is shown in Figure 8 (curves 3 and 4). The most important variable appears to be MMD3 (mass median diameter for third component); increasing this variable decreases the solution time. In addition, increasing GSD3 (geometric standard deviation for diameter of third component) and χ (dynamic shape factor) also decreases the solution time, while increasing ϵ (turbulence dissipation rate) increases solution time. Properties of the third aerosol component are important in influencing computational time because it is added to the system at a significantly higher rate than the other two components (i.e., see SR1, SR2 and SR3 in Table I). Increasing MMD3 results in more mass being associated with larger particles; in turn, this results in less rapid agglomeration, longer time steps by the differential equation solver, and hence, lower overall solution time. Similarly, increasing GSD3 tends to move mass to larger particles and hence reduce solution time. Increasing χ decreases the rate of agglomeration; this results in longer time steps by the differential equation and lower overall solution time. In contrast, increasing ϵ results in more rapid agglomeration, shorter time steps and larger overall solution time.

As all the regressions in Table III have R^2 values below 0.6, they are not completely successful in accounting for the observed variation in CPU time required to solve the MAEROS equations. This lack of success is probably due in part to the discretization of solution time on the basis of the number of steps required by the differential equation solver and in part to the summation of solution times (e.g., the solution time to 10 sec was taken to be the solution time from 0 sec to 1 sec, plus the solution time from 1 sec to 5 sec, plus the solution time from 5 sec to 10 sec). Both of these processes have effects on the analyzed solution times that tend to obscure the influence of variables in Table I.

The regression analyses for the suspended concentrations of the three components are presented in Tables IV, V and VI. For each component, the most important variables are the source rate for that component (i.e., SR1, SR2 or SR3), ϵ (turbulence dissipation rate) and γ (agglomeration shape factor). Increasing a source rate increases the corresponding component concentration, while increasing ϵ and γ, decreases concentration by increasing the rate at which agglomeration is taking place. Most of the other variables selected in the regressions are related to agglomeration and tended to decrease suspended concentration as their values increased.

7. Discussion. A computational test problem involving a three component aerosol in the upper plenum of a pressurized water reactor is used to investigate various characteristics of the MAEROS aerosol model. For this problem, the use of 5 sections and section boundaries from 0.1E-6 m to 50.E-6 m was found to be adequate; model formulations using larger numbers of sections and wider overall section boundaries were more time-consuming computationally but yielded similar results. For the preceding formulation, the solution from 0 sec to 10 sec was approximately 270 to 450 times faster than real time, while the solution from 0 sec to 30 sec was approximately 390 to 1100 times faster than real time. Based on present knowledge of the MELCOR code system, this range of computational times is felt to be acceptable for the aerosol problem under consideration. It is likely that MELCOR will use time steps of approximately 10 sec for primary system problems.

An additional test was made to determine if a significant reduction in computational time could be made by coalescing the three aerosol components under consideration into a single component. For 10 sections and overall section boundaries of 0.1E-6 m to 50.E-6 m, this reduction from a system of 30 differential equations to a system of 10 differential equations lead to a 30% decrease in solution time.

Most of this presentation has dealt with the solution time required by different formulations of the system of differential equations underlying MAEROS. However, a significant amount of time is required to evaluate the coefficients used in this system (i.e., compare the distributions of time to evaluate coefficients in Figure 7 with the distributions of solution time in Figures 8, 2 and 9). For example, the time to evaluate the coefficients is often 4 to 6 times the time required to solve the associated system from t=0 sec to t=30 sec Thus, if the coefficients must be recalculated often, this could require more computational time than solving the associated systems of differential equations. On the other hand, if the coefficients are evaluated infrequently, then the time required in their calculation would probably be small relative to that required to solve the equations. In this regard, the MAEROS program (1) contains an interpolation procedure which permits a quick recalculation of the coefficients for changes in temperature and pressure. However, in the presented analyses, temperature and pressure were not found to be very important in influencing the aerosol under consideration; other variables had larger effects. The interpolation procedure to recalculate coefficients for changes in temperature and pressure was not used in this analysis; rather, 50 sets of coefficients (i.e., one for each Latin hypercube sample vector) were calculated for each computational variation of the aerosol problem.

In the implementation of the MAEROS model in MELCOR, it is planned to decompose the coefficients associated with the equation in (1) in a way which permits the direct use of temperatures and pressures calculated in the thermal-hydraulics submodels. This will obviate the need to recalculate coefficients for changes in temperature and pressure. However, the need may remain to handle coefficient variability due to changes in other system properties.

Overall, the variability in computational time was not large. For a specified number of sections and a given pair of lower and upper section boundaries, the largest observed time to evaluate the model coefficients was about 1.2 to 1.3 times the smallest observed value. Similarly, for solution time over various intervals, the largest observed time was 2 to 4 times the smallest observed value. Thus, for problems of the type considered here, it appears that large swings in computational time do not take place for perturbations in system properties (i.e., the variables listed in Table I). Such stability is very desirable in an often called module of a large code system such as MELCOR.

A sensitivity analysis based on stepwise regression was performed to determine which of the variables in Table I are most important in influencing computational time and suspended aerosol concentration. The most important variables for time to compute the MAEROS coefficients were χ (dynamic shape factor) and ε (turbulence dissipation rate). Overall, MMD3 (mass median diameter of third aerosol component), ε and GSD3 (geometric standard deviation of third aerosol component) were most important in influencing solution time. For suspended aerosol

mass, the most important variables were the source rate of the particular aerosol component under consideration, ε and γ (agglomeration shape factor).

Sensitivity analysis results provide useful guidance for additional study. For example, a relatively small subset of the variables in Table I dominates the uncertainty in the suspended concentrations of the three aerosol components (see Tables IV, V and VI). To reduce uncertainty in these concentrations, efforts should be focused on reducing the uncertainty in the most important independent variables (i.e., SR1, SR2, SR3, γ, ε). If the uncertainty in such variables cannot be controlled, there is little to be gained by reducing the uncertainty in other less important variables.

Computational time for this problem appears to be acceptable for the MELCOR code system. If such were not the case, a productive area for additional investigation would be any variables which affected computational time but did not influence dependent variables of interest. For example, MMD3 (mass median diameter of third aerosol component) has a larger effect on computational time than it has on aerosol concentration.

This analysis employed techniques based on Latin hypercube sampling and stepwise regression. It is felt that this provides an effective approach to investigating model complexity. First, the use of Latin hypercube sampling assures consideration of both the full range of each variable and a wide variety of variable combinations. Second, the use of stepwise regression makes it possible to determine the variables which are affecting quantities of interest. The presented techniques should be applicable for systematically investigating complexity problems for a variety of models.

References

1. F. Gelbard, "MAEROS User Manual," NUREG/CR-1391, SAND80-0822, Sandia National Laboratories (1982).

2. F. Gelbard and J. H. Seinfeld, "Simulation of Multicomponent Aerosol Dynamics," J. Colloid Interface Sci., 78, 485 (1980).

3. J. L. Sprung, D. C. Aldrich, D. J. Alpert and G. G. Weigand, "Overview of the MELCOR Risk Code Development Program," in Proceedings of the International Meeting on Light Water Reactor Severe Accident Evaluation, Cambridge, MA, August 28-September 1, 1983, p. TS-10.1-1 (1983).

4. K. D. Bergeron, M. J. Clauser, B. D. Harrison, K. K. Murata, P. E. Rexroth, F. J. Schelling, F. W. Sciacca, M. E. Senglaub, P. R. Shire and W. Trebilcock, "User's Manual for CONTAIN, A Computer Code for Severe Nuclear Reactor Accident Containment Analysis," NUREG/CR-4085, SAND84-1204, Sandia National Laboratories (1985).

5. J. C. Helton, R. L. Iman, J. D. Johnson and C. D. Leigh, "Uncertainty and Sensitivity Analysis of a Model for Multicomponent Aerosol Dynamics," NUREG/CR-4342, SAND84-1307, Sandia National Laboratories (1985).

6. M. D. McKay, W. J. Conover and R. J. Beckman, "A Comparison of Three Methods for Selecting Values of Input Variables in the Analysis of Output from a Computer Code," Technometrics, 21, 239 (1979).

7. R. L. Iman and M. J. Shortencarier, "A FORTRAN 77 Program and User's Guide for the Generation of Latin Hypercube and Random Samples for Use with Computer Models," NUREG/CR-3624, SAND83-2365, Sandia National Laboratories (1984).

8. R. L. Iman and W. J. Conover, "A Distribution-Free Approach to Inducing Rank Correlation Among Input Variables," Communications in Statistics, B11, 311 (1982).

9. L. F. Shampine and H. A. Watts, "Practical Solution of Ordinary Differential Equations by Runge-Kutta Methods," SAND76-0585, Sandia National Laboratories (1976).

10. S. W. Webb, personal communication (1984).

11. R. L. Iman, J. M. Davenport, E. L. Frost and M. J. Shortencarier, "Stepwise Regression with PRESS and Rank Regression (Program User's Guide)," SAND79-1472, Sandia National Laboratories (1980).

12. R. L. Iman and W. J. Conover, "The Use of the Rank Transform in Regression," Technometrics, 21, 499 (1979).

13. D. M. Allen, "The Prediction Sum of Squares as a Criterion for Selecting Predictor Variables," Report No. 23, Department of Statistics, University of Kentucky (1971).

14. R. L. Iman and J. C. Helton, "A Comparison of Uncertainty and Sensitivity Analysis Techniques for Computer Models," NUREG/CR-3904, SAND84-1461, Sandia National Laboratories (1985).

15. R. L. Iman, J. C. Helton and J. E. Campbell, "An Approach to Sensitivity Analysis of Computer Models, Part 1. Introduction, Input Variable Selection and Preliminary Variable Assessment," J. Quality Tech., 13, 174 (1981).

16. R. L. Iman, J. C. Helton and J. E. Campbell, "An Approach to Sensitivity Analysis of Computer Models, Part 2. Ranking of Input Variables, Response Surface Validation, Distribution Effect and Technique Synopsis," J. Quality Tech., 13, 232 (1981).

Table I Variables for Upper Plenum Test Problem. Components 1, 2 and 3 correspond to CsI, CsOH, and other aerosol materials, respectively.

Variable	Definition	Range	Distribution	Restrictions
GSD1	Geometric standard deviation for diameter of first component (unitless)	1.3-4.	uniform	--
MMD1	Mass median diameter for first component (m)	0.01E-6-5.E-6	log uniform	0.5 rank correlation with SR1
SR1	Total mass source rate for first component (kg/sec)	0.01-0.03	uniform	0.5 rank correlation with MMD1
RD1	Release duration for first component (sec)	2.34E3-9.42E3	uniform	--
GSD2	Geometric standard deviation for diameter of second component (unitless)	1.3-4.	uniform	--
MMD2	Mass median diameter for second component (m)	0.01E-6-5.E-6	log uniform	0.5 rank correlation with SR2
SR2	Total mass source rate for second component (kg/sec)	0.06-0.21	uniform	0.5 rank correlation with MMD2
RD2	Release duration for second component (sec)	2.34E3-9.42E3	uniform	--
GSD3	Geometric standard deviation for diameter of third component (unitless)	1.3-4.	uniform	--
MMD3	Mass median diameter for third component (m)	0.01E-6-5.E-6	log uniform	0.5 rank correlation with SR3
SR3	Total mass source rate for third component (kg/sec)	0.76-2.62	uniform	0.5 rank correlation with MMD3
RD3	Release duration for third component (sec)	2.34E3-9.46E3	uniform	--
T	Temperature (K)	800.-1800.	uniform	--
P	Pressure (Pa)	1.6E7-1.8E7	uniform	--
RCV	Ratio of ceiling area to volume (m^{-1})	3.-9.	uniform	--

Table I Variables for Upper Plenum Test Problem (continued).

Variable	Definition	Range	Distribution	Restrictions
RFV	Ratio of floor area to volume (m^{-1})	3.-9.	uniform	--
RWV	Ratio of wall area to volume (m^{-1})	5.-50.	uniform	--
χ	Dynamic shape factor (unitless)	1.-7.	uniform	$\chi \leq \gamma$
δ	Diffusion boundary layer thickness (m)	5.E-5-8.E-3	log uniform	--
ρ	Particle material density (kg/m^3)	2.E3-8.E3	normal	--
C_T	Constant associated with thermal accommodation coefficient (unitless)	1.-3.	uniform	--
γ	Agglomeration shape factor (unitless)	1.-7.	uniform	$\gamma \geq \chi$
ST	Probability sticking factor (unitless)	0.5-1.	uniform	--
∇K	Temperature gradient (K/m)	1.E3-5.E4	log uniform	--
κ	Ratio of thermal conductivity of gas to that of particle (unitless)	0.05-1.	triangular with an apex at 0.5	--
ϵ	Turbulence dissipation rate (m^2/sec^3)	0.001-0.1	log uniform	--
MW	Molecular weight of gas (kg/kg-mole)	2.-18.	uniform	--

Table II Regression Analyses for CPU Time (sec) to Compute MAEROS Coefficients for Upper Plenum Test Problem with 5 Sections and Section Boundaries of 0.1E-6 m to 50.E-6 m.

	RAW			RANK		
Step	Var[a]	SRC[b]	R^{2c}	Var[a]	SRC[b]	R^{2c}
1	χ	-0.70	0.51	χ	-0.60	0.49
2	ϵ	-0.41	0.68	ϵ	-0.56	0.78
3				γ	-0.21	0.80
4				∇K	-0.16	0.83
5				MW	-0.15	0.85
6				ρ	0.14	0.87

a Variables listed in the order that they entered the regression model.

b Standardized regression coefficients for final regression model.

c R^2 value with entry of each successive variable into the regression model.

Table III Regression Analyses for CPU Time (sec) to Solve MAEROS Equations with RKF45 (RELTOL = 10^{-3} and ABTOL = 10^{-20}) for Upper Plenum Test Problem with 5 Sections, 3 Components and Section Boundaries of 0.1E-6 m to 50.E-6 m. Notation is the same as in Table II.

	RAW			RANK		
Step	Var	SRC	R^2	Var	SRC	R^2
1[a]	MMD3	-0.57	0.31	MMD3	-0.51	0.29
2	GSD3	-0.36	0.44	ϵ	0.34	0.41
3	ϵ	0.29	0.53	GSD3	-0.26	0.48
4	SR1	-0.25	0.59	SR1	-0.25	0.54
1[b]	MMD3	-0.80	0.32	MMD3	-0.65	0.42
2	χ	-0.31	0.41			
3	GSD3	-0.30	0.49			
4	SR3	0.32	0.57			

a Solution time: 0 sec to 10 sec.

b Solution time: 0 sec to 30 sec.

Table IV Regression Analyses for Suspended Concentration (kg/m^3) of First Aerosol Component (CsI). Notation is the same as in Table II.

	RAW			RANK		
Step	Var	SRC	R^2	Var	SRC	R^2
1[a]	SR1	0.57	0.39	SR1	0.63	0.37
2	ϵ	-0.44	0.57	ϵ	-0.49	0.57
3	γ	-0.46	0.74	γ	-0.40	0.71
4	MMD3	-0.25	0.80	SR3	-0.23	0.76
5	ST	-0.16	0.83			
1[b]	γ	-0.63	0.39	SR1	0.59	0.31
2	SR1	0.45	0.61	ϵ	-0.53	0.55
3	ϵ	-0.35	0.72	γ	-0.45	0.73
4	MMD3	-0.22	0.77	SR3	-0.24	0.79
5				T	0.19	0.82
6				ST	-0.15	0.85

a Suspended concentration at 10 sec.

b Suspended concentration at 30 sec.

Table V Regression Analyses for Suspended Concentration (kg/m^3) of Second Aerosol Component (CsOH). Notation is the same as in Table II.

	RAW			RANK		
Step	Var	SRC	R^2	Var	SRC	R^2
1[a]	SR2	0.69	0.41	SR2	0.76	0.38
2	ϵ	-0.49	0.64	ϵ	-0.54	0.62
3	γ	-0.40	0.77	γ	-0.45	0.78
4	MMD3	-0.18	0.80	MMD3	-0.19	0.82
5				ST	-0.18	0.85
6				MMD2	-0.18	0.87
1[b]	γ	-0.61	0.29	SR2	0.68	0.28
2	SR2	0.56	0.57	γ	-0.57	0.51
3	ϵ	-0.44	0.75	ϵ	-0.51	0.76
4	MMD3	-0.19	0.78	ST	-0.21	0.80
5				MMD2	-0.21	0.84
6				SR3	-0.16	0.86

a Suspended concentration at 10 sec.

b Suspended concentration at 30 sec.

Table VI Regression Analyses for Suspended Concentration (kg/m^3) of Third Aerosol Component (Other materials). Notation is the same as in Table II.

	RAW			RANK		
Step	Var	SRC	R^2	Var	SRC	R^2
1[a]	SR3	0.66	0.28	ϵ	-0.57	0.30
2	ϵ	-0.54	0.54	SR3	0.54	0.53
3	γ	-0.42	0.68	γ	-0.41	0.68
4	MMD3	-0.33	0.77	ST	-0.21	0.73
5	ST	-0.22	0.82	MMD3	-0.21	0.77
1[b]	γ	-0.63	0.41	ϵ	-0.56	0.26
2	ϵ	-0.46	0.58	γ	-0.52	0.55
3	SR3	0.47	0.70	SR3	0.46	0.68
4	MMD3	-0.29	0.76	ST	-0.21	0.73
5	ST	-0.18	0.79	MMD3	-0.24	0.77
6				MW	-0.21	0.81
7				T	0.20	0.85
8				ρ	0.16	0.87

a Suspended concentration at 10 sec.

b Suspended concentration at 30 sec.

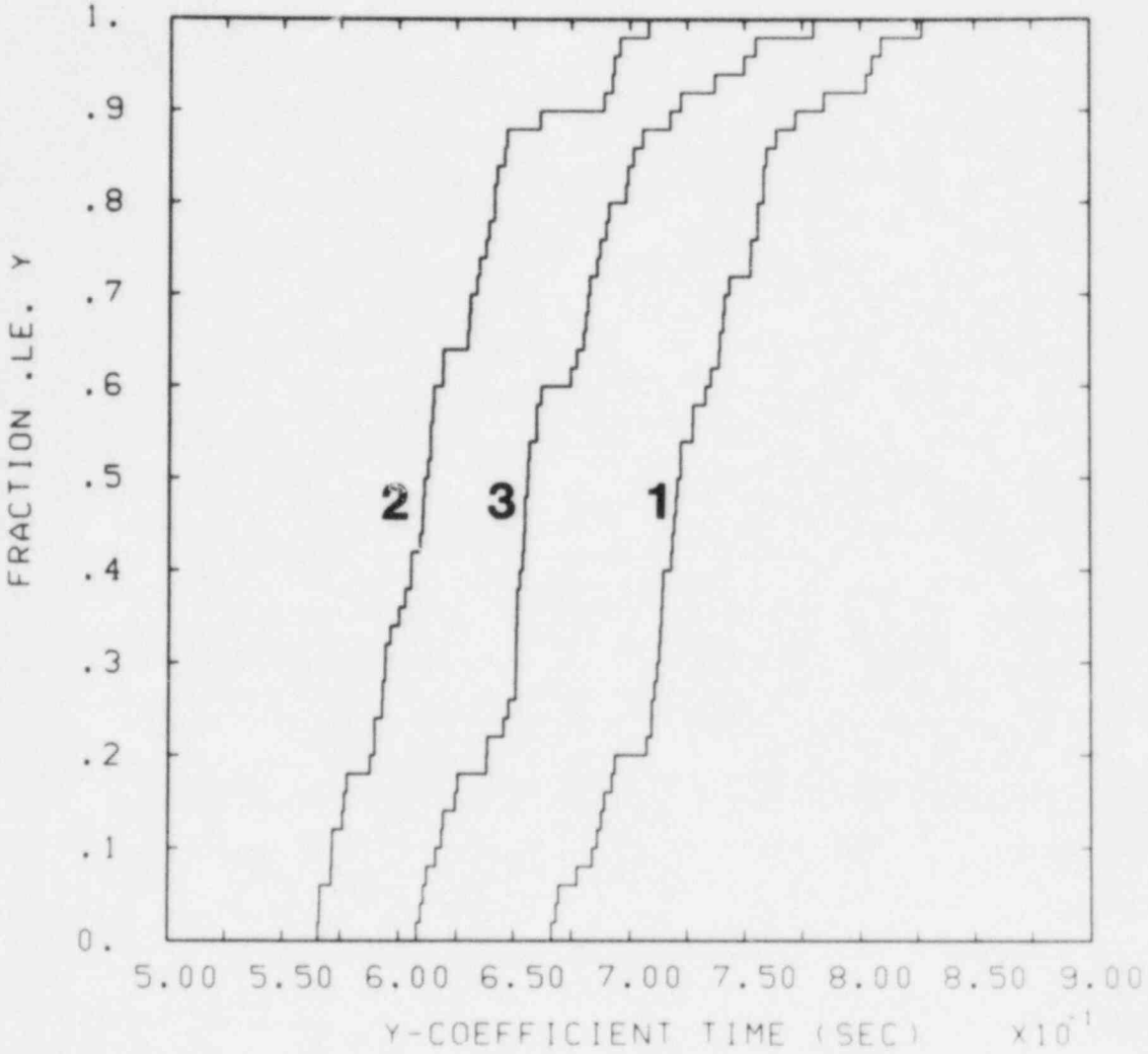

Figure 1 Distribution of CPU Time (sec) to Calculate One Set of MAEROS Coefficients for Upper Plenum Test Problem with 10 Sections and Different Section Boundaries (1 ~ 0.01E-6 m to 50.E-6 m, 2 ~ 0.1E-6 m to 50.E-6 m, 3 ~ 0.1E-6 m to 100.E-6 m). In this and other figures, the scale factor (i.e., 10^{-1}) is applied to the numbers on the associated axis (i.e., the range on the x-axis is from 0.5 to 0.9).

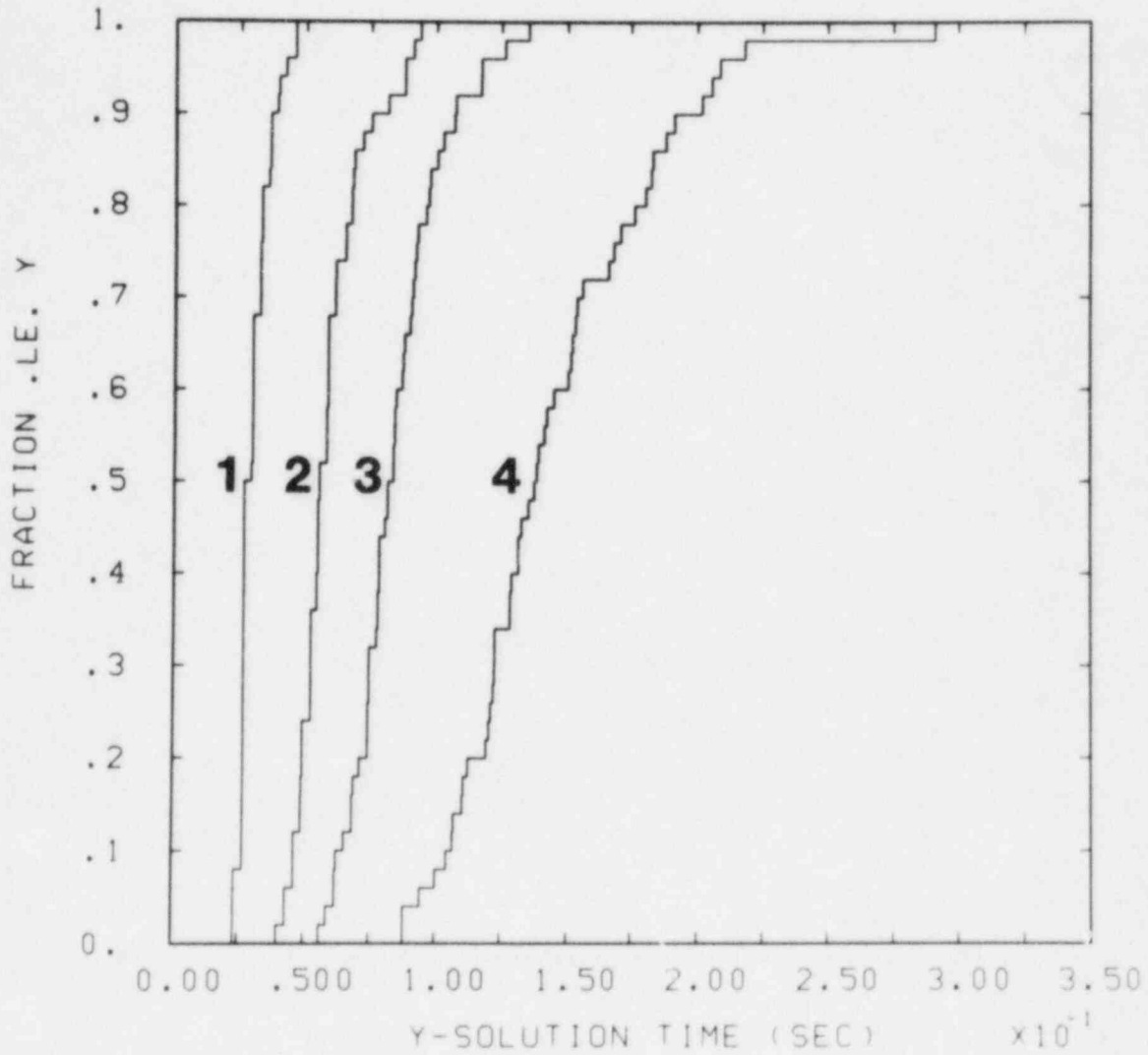

Figure 2 Distribution of CPU Time (sec) for Solution of MAEROS Equations with RKF45 (RELTOL = 10^{-3} and ABTOL = 10^{-20}) for Upper Plenum Test Problem with 10 Sections, 3 Components and Section Boundaries of 0.1E-6 m to 50.E-6 m (1 ~ 0 sec to 1 sec, 2 ~ 0 sec to 5 sec, 3 ~ 0 sec to 10 sec, 4 ~ 0 sec to 30 sec).

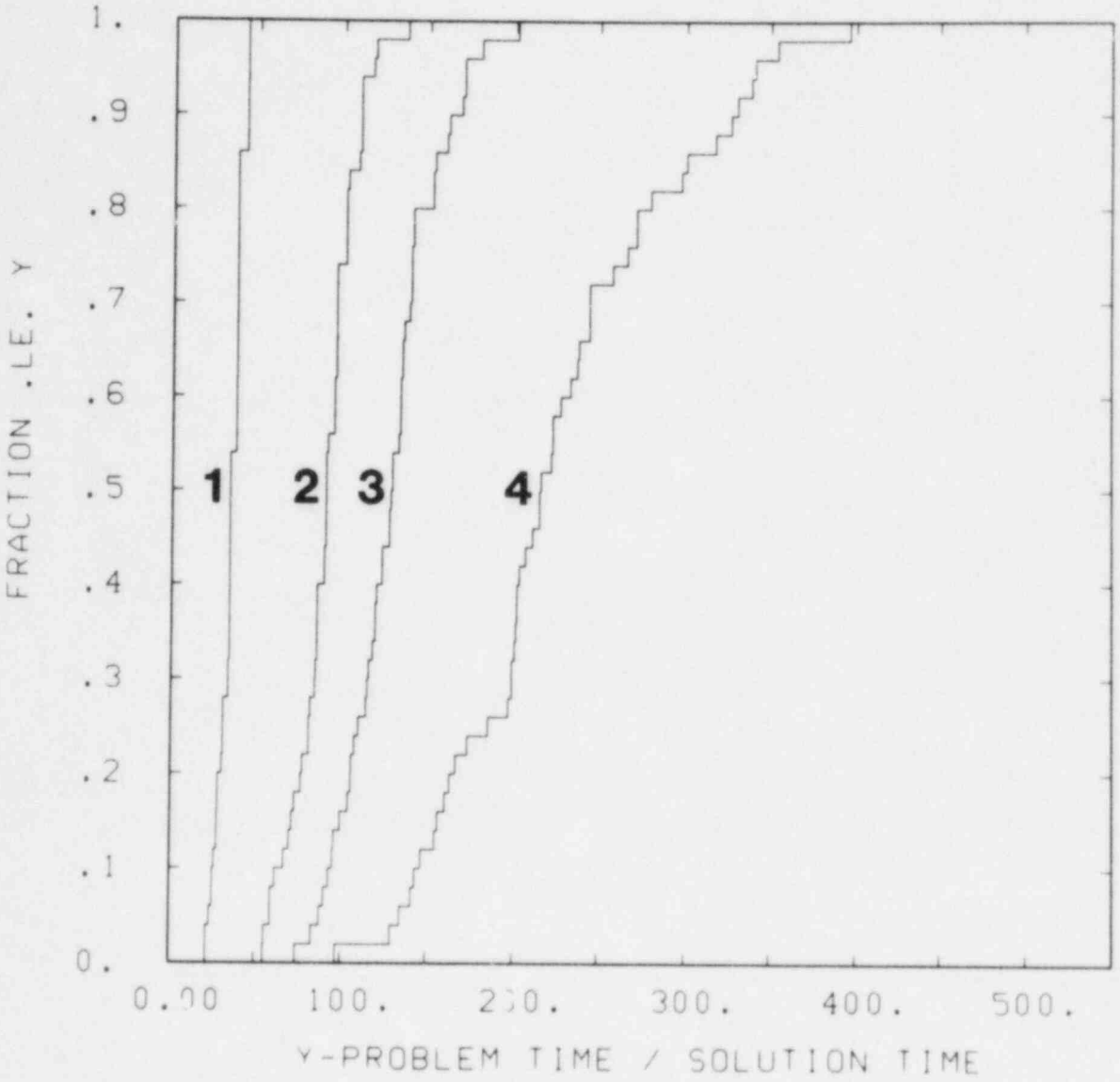

Figure 3 Distribution of Problem Time/Solution Time for Solution of MAEROS Equations with RKF45 (RELTOL = 10^{-3} and ABTOL = 10^{-20}) for Upper Plenum Test Problem with 10 Sections, 3 Components and Section Boundaries of 0.1E-6 m to 50.E-6 m (1 ~ 0 sec to 1 sec, 2 ~ 0 sec to 5 sec, 3 ~ 0 sec to 10 sec, 4 ~ 0 sec to 30 sec).

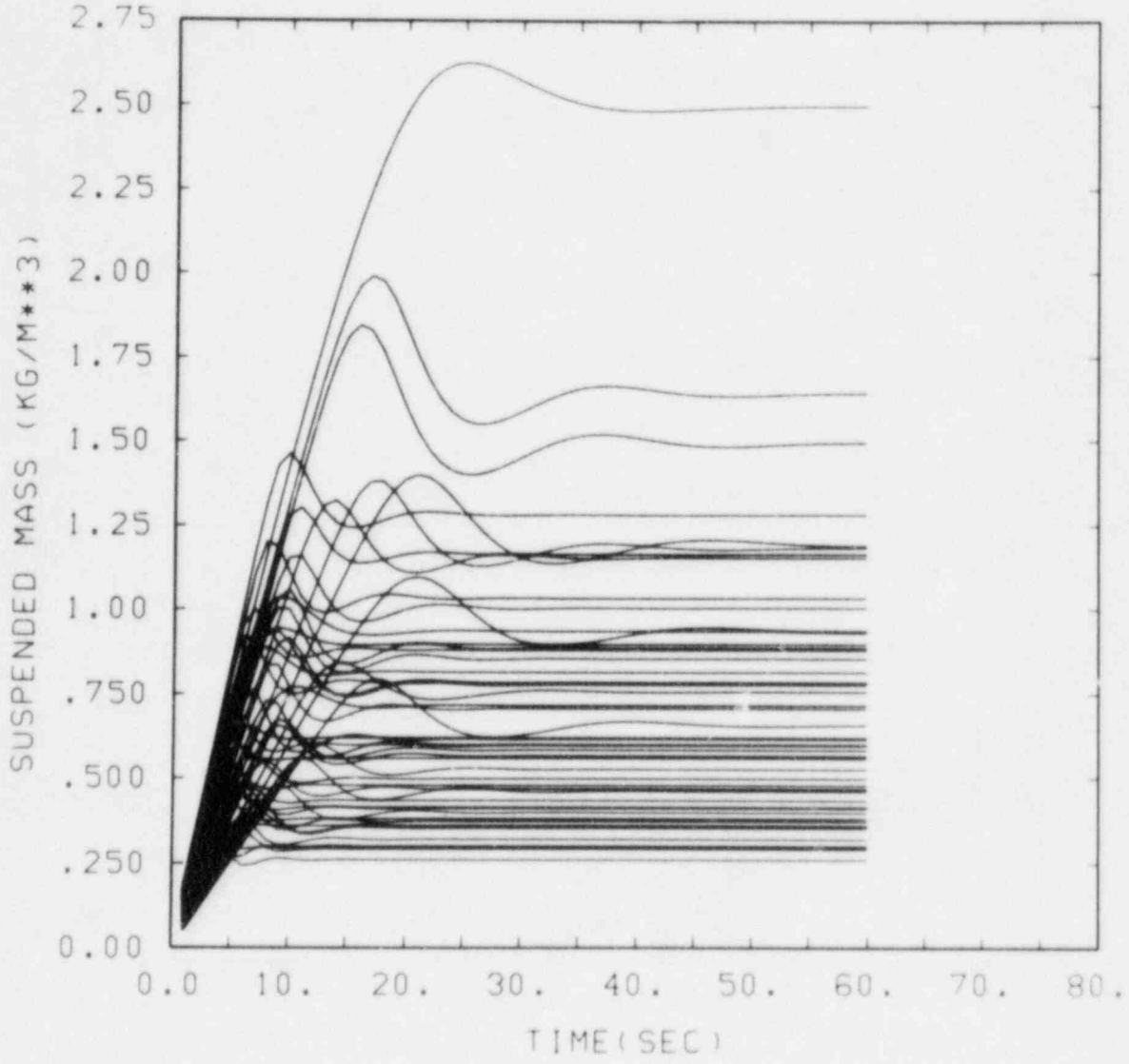

Figure 4 Time-Dependent Behavior of Third Aerosol Component (other materials) for Upper Plenum Test Problem. Each curve in this figure corresponds to the prediction associated with one Latin hypercube sample vector. The behavior of the other two components was similar.

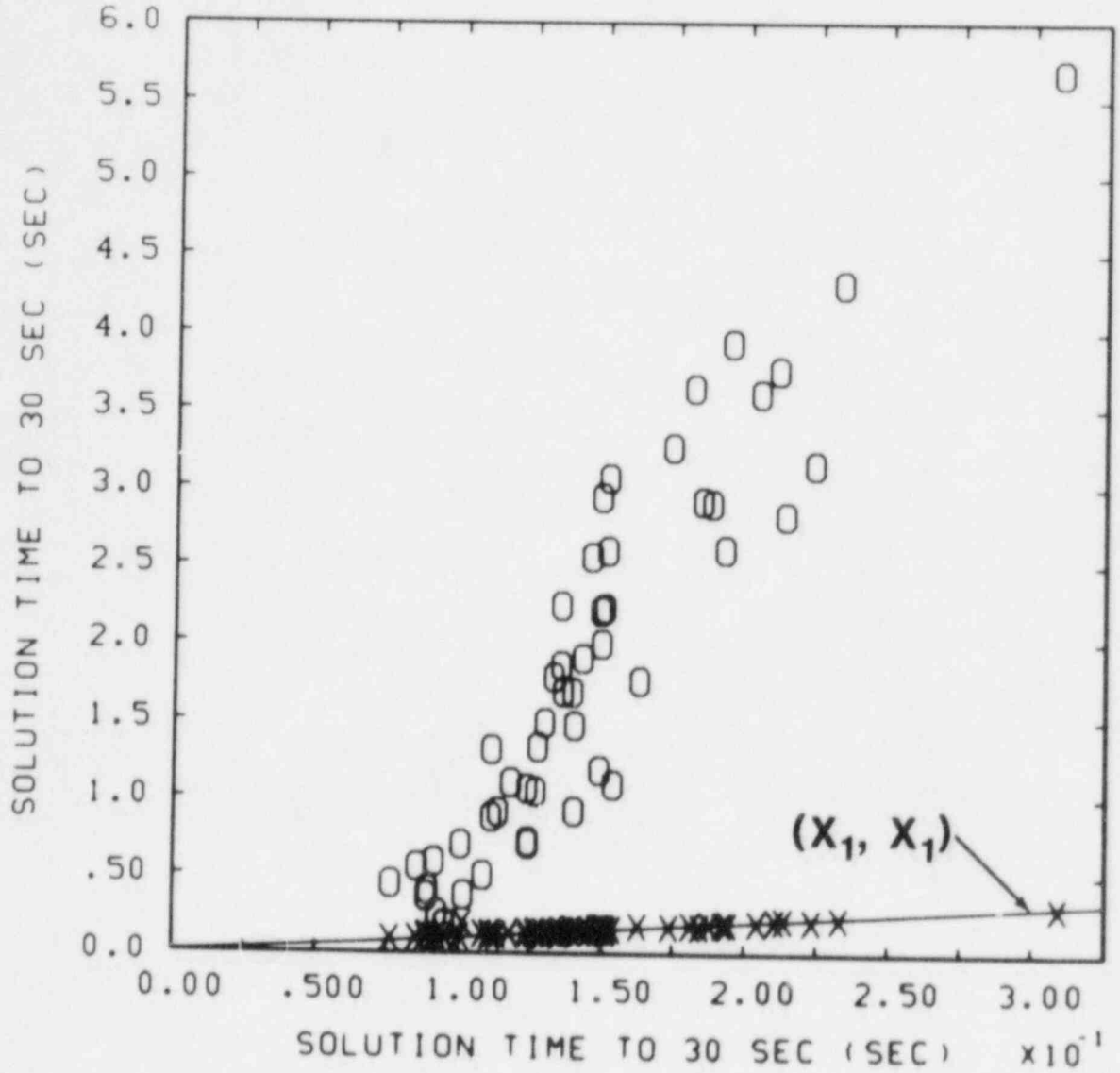

Figure 5 Solution Time (sec) to 30 sec for MAEROS Equations with RKF45 (RELTOL = 10^{-3} and ABTOL = 10^{-20}) for Upper Plenum Test Problem with 10 Sections, 3 Components and Different Section Boundaries (X ~ (X_1, Y_1) and O ~ (X_1, Y_2), where X_1, Y_1 and Y_2 denote solution times with boundaries of 0.1E-6 m to 50.E-6 m, 0.1E-6 m to 100.E-6 m, and 0.01E-6 m to 50.E-6 m, respectively).

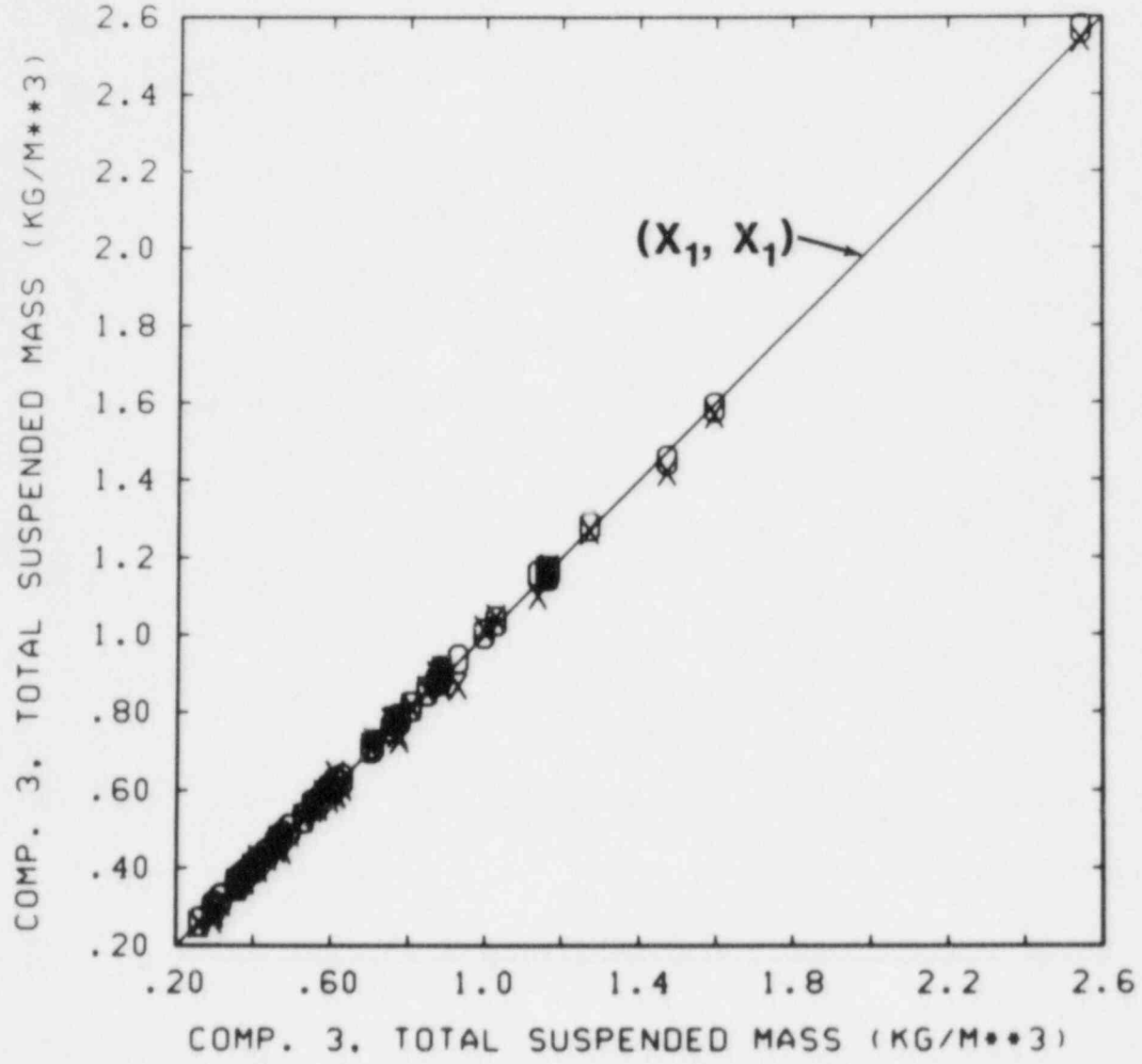

Figure 6 Total Suspended Mass (kg/m^3) of Third Component (other materials) at 30 sec for Upper Plenum Test Problem with 10 Sections and Different Section Boundaries (X ~ (X_1, Y_1) and 0 ~ (X_1, Y_2), where X_1, Y_1 and Y_2 denote suspended mass for boundaries of 0.1E-6 m to 50.E-6 m, 0.1E-6 m to 100.E-6 m, and 0.01E-6 m to 50.E-6 m, respectively).

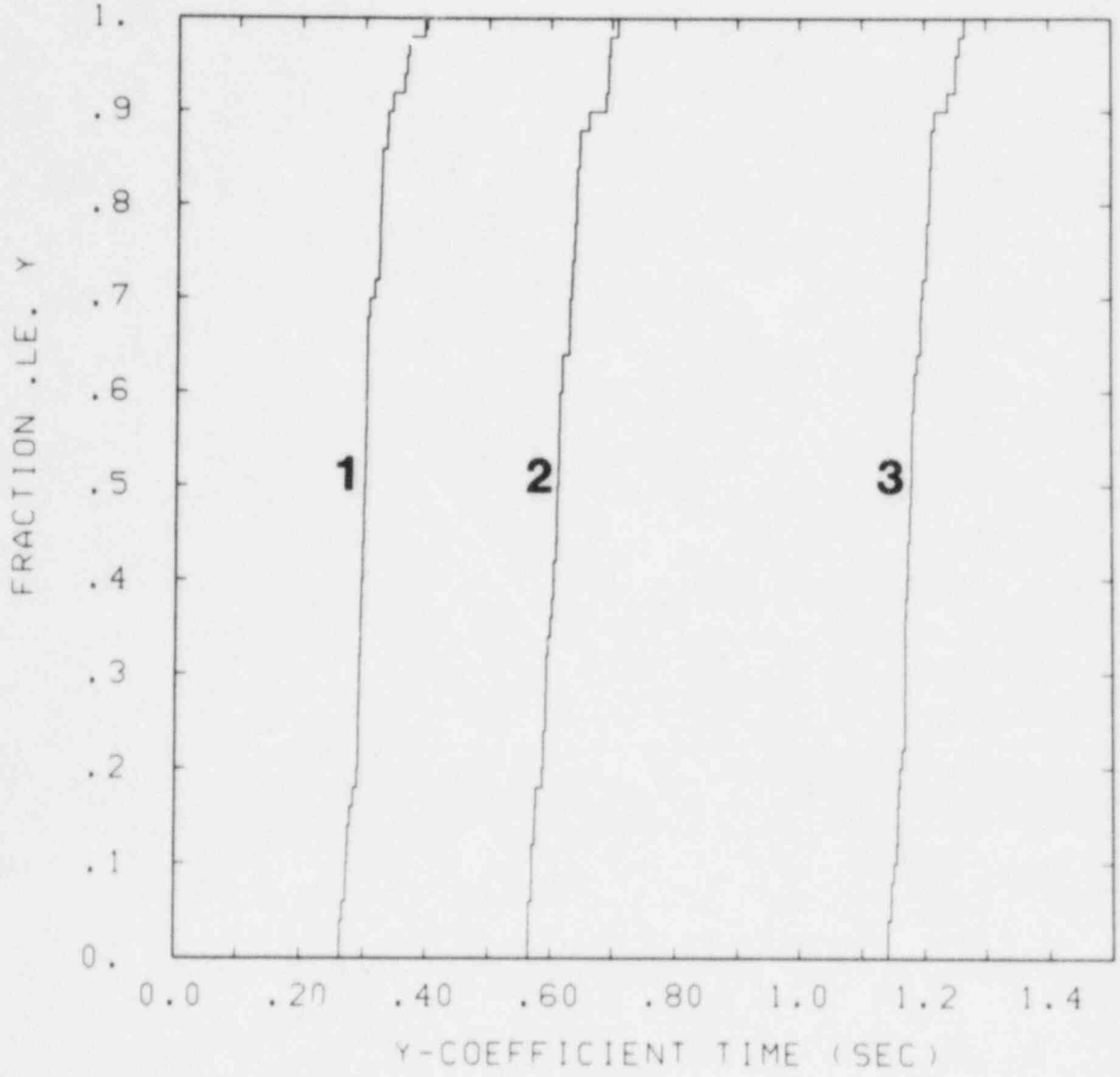

Figure 7 Distribution of CPU Time (sec) to Calculate One Set of MAEROS Coefficients for Upper Plenum Test Problem with Section Boundaries of 0.1E-6 m to 50.E-6 m and Different Numbers of Sections (1 ~ 5 sections, 2 ~ 10 sections, 3 ~ 15 sections).

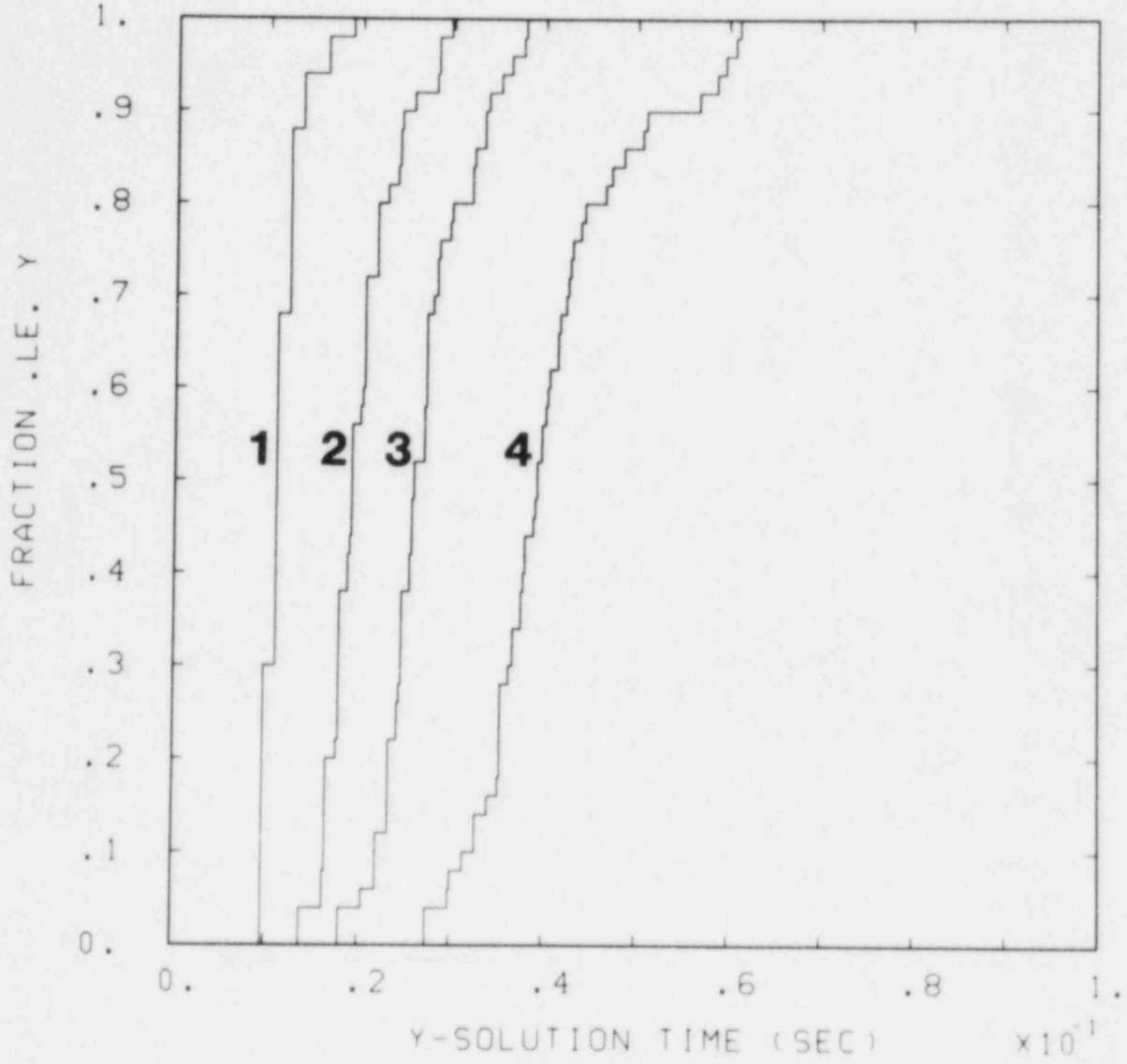

Figure 8 Distribution of CPU Time (sec) for Solution of MAEROS Equations with RKF45 (RELTOL = 10^{-3} and ABTOL = 10^{-20}) for Upper Plenum Test Problem with 5 Sections, 3 Components and Section Boundaries of 0.1E-6 m to 50.E-6 m (1 ~ 0 sec to 1 sec, 2 ~ 0 sec to 5 sec, 3 ~ 0 sec to 10 sec, 4 ~ 0 sec to 30 sec).

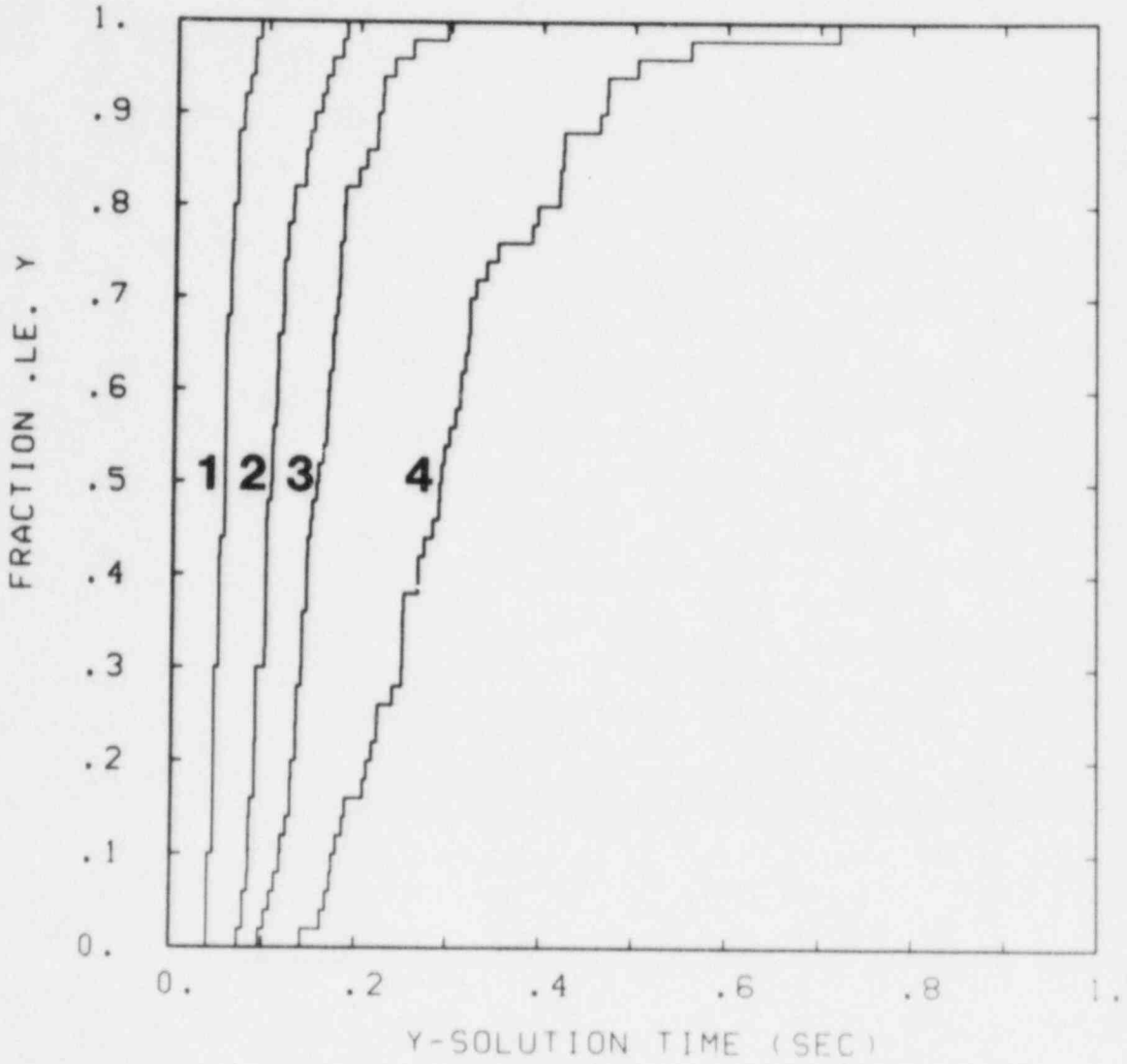

Figure 9 Distribution of CPU Time (sec) for Solution of MAEROS Equations with RKF45 (RELTOL = 10^{-3} and ABTOL = 10^{-20}) for Upper Plenum Test Problem with 15 Sections, 3 Components and Section Boundaries of 0.1E-6 m to 50.E-6 m (1 ~ 0 sec to 1 sec, 2 ~ 0 sec to 5 sec, 3 ~ 0 sec to 10 sec, 4 ~ 0 sec to 30 sec).

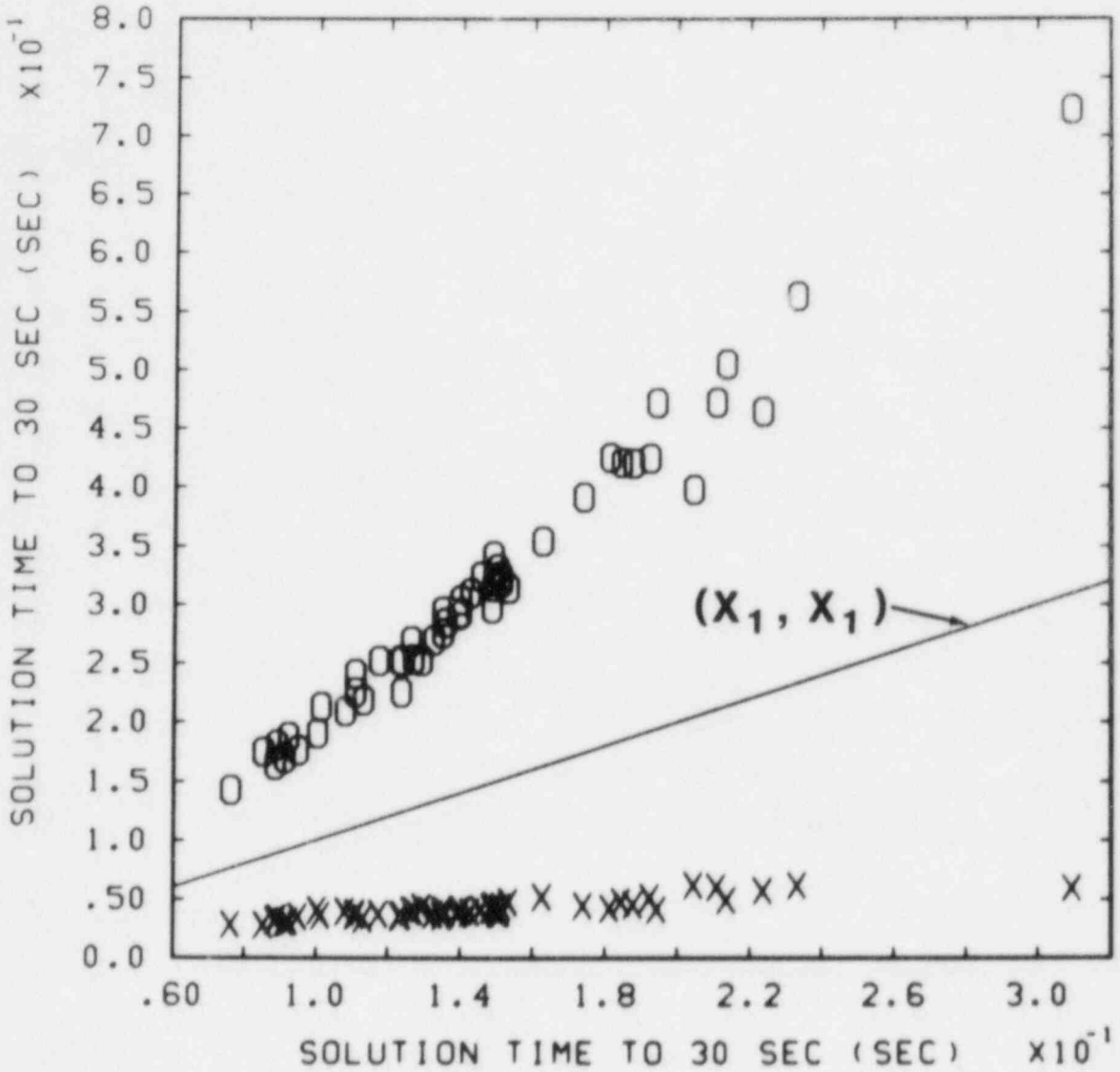

Figure 10 Solution Time (sec) to 30 sec for MAEROS Equations with RKF45 (RELTOL = 10^{-3} and ABTOL = 10^{-20}) for Upper Plenum Test Problem with 3 Components, Section Boundaries of 0.1E-6 m to 50.E-6 m, and Different Numbers of Sections (X ~ (X_1, Y_1) and O ~ (X_1, Y_2), where X_1, Y_1 and Y_2 denote solution times with 10, 5 and 15 sections, respectively).

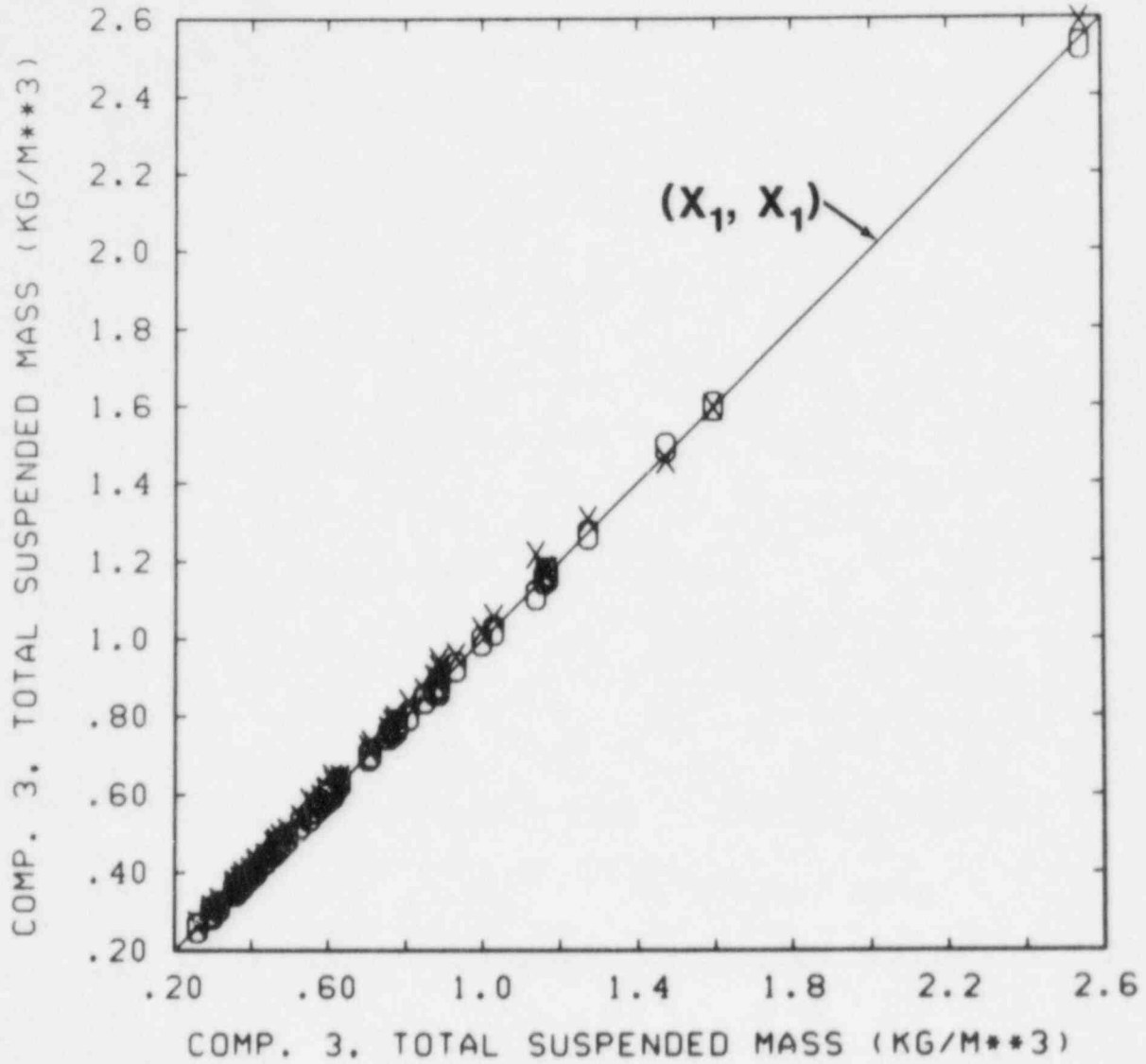

Figure 11 Total Suspended Mass (kg/m^3) of Third Component (other materials) at 30 sec for Upper Plenum Test Problem with Section Boundaries of 0.1E-6 m to 50.E-6 m and Different Numbers of Sections (X ~ (X_1, Y_1) and 0 ~ (X_1, Y_2), where X_1, Y_1 and Y_2 denote suspended mass for 10, 5 and 15 sections, respectively).

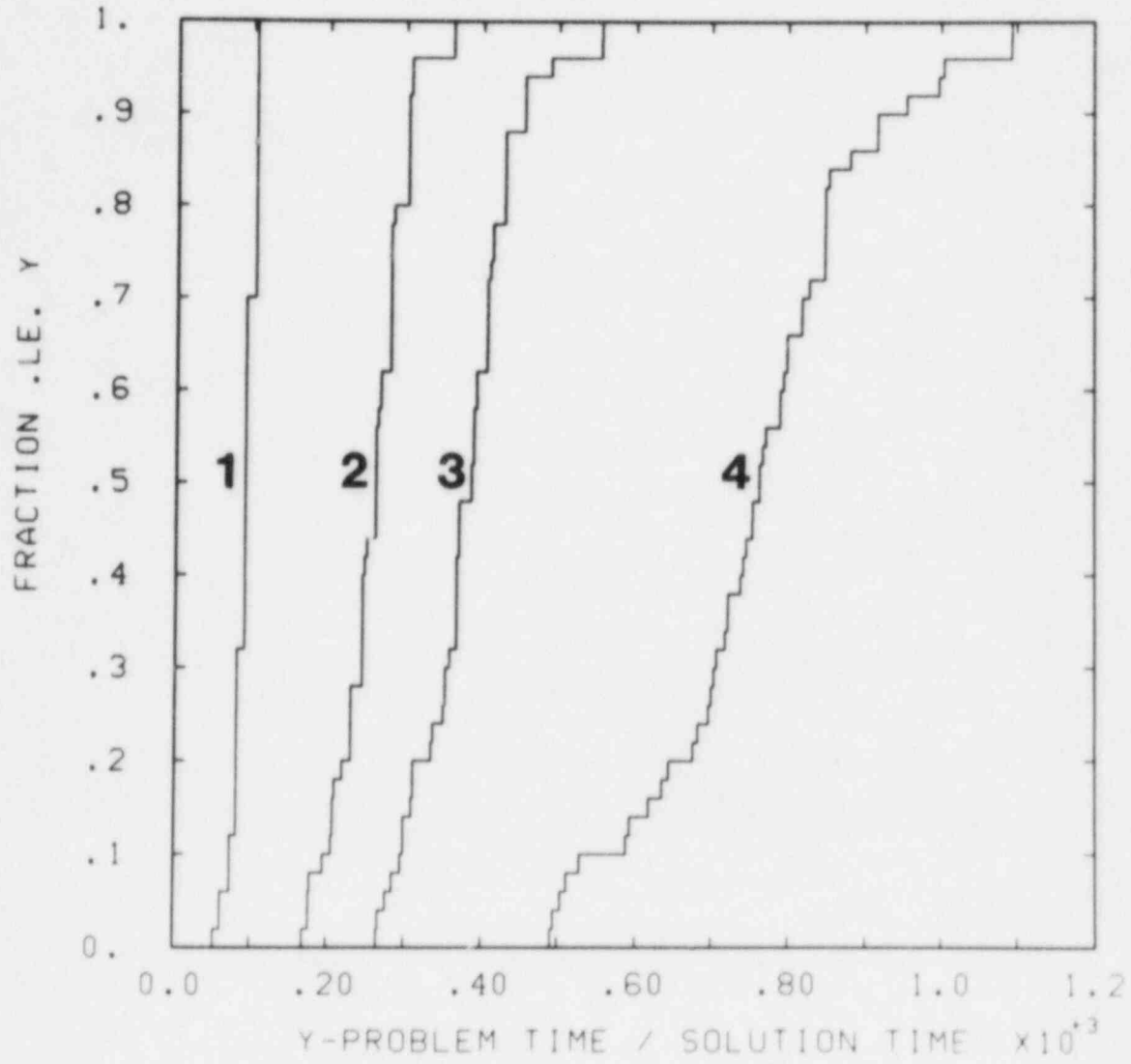

Figure 12 Distribution of Problem Time/Solution Time for Solution of MAEROS Equations with RKF45 (RELTOL = 10^{-3} and ABTOL = 10^{-20}) for Upper Plenum Test Problem with 5 Sections, 3 Components and Section Boundaries of 0.1E-6 m to 50.E-6 m (1 ~ 0 sec to 1 sec, 2 ~ 0 sec to 5 sec, 3 ~ 0 sec to 10 sec, 4 ~ 0 sec to 30 sec).

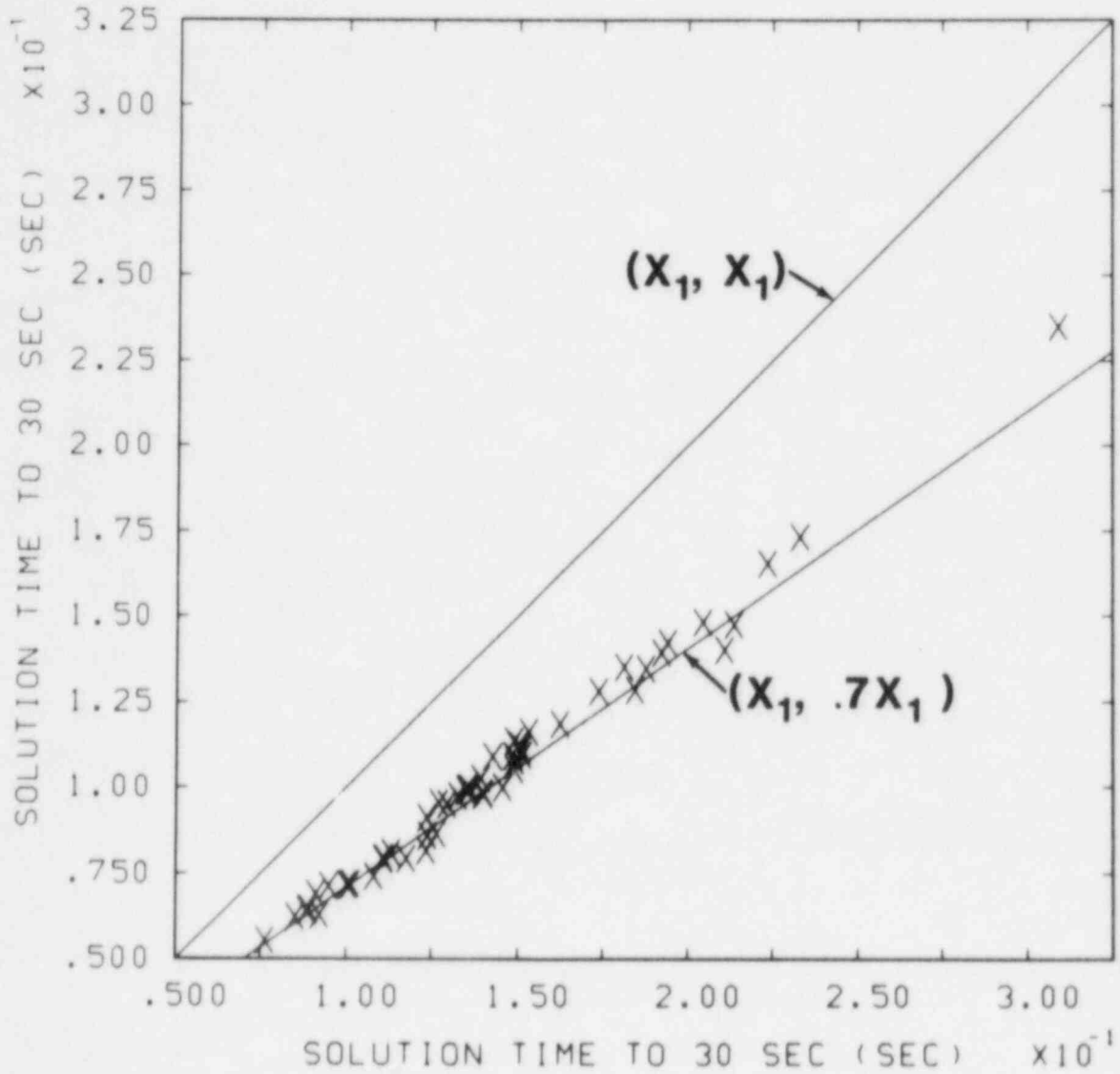

Figure 13 Solution Time (sec) to 30 sec for MAEROS Equations with RKF45 (RELTOL = 10^{-3} and ABTOL = 10^{-20}) for Upper Plenum Test Problem with 10 Sections, Section Boundaries of 0.1E-6 m to 50.E-6 m, and Different Numbers of Components ($X \sim (X_1, Y_1)$, where X_1 and Y_1 correspond to 3 and 1 components, respectively).

U. S. Government Printing Office
Receiving Branch (Attn: NRC Stock)
8610 Cherry Lane
Laurel, MD 20707
250 copies for RG

USNRC (5)
Division of Risk Analysis and Operations
Washington, DC 20555
M.Cunningham
J. Johnson
L. Lancaster
T. Margulies
D. Rasmuson

Los Alamos National Laboratory (3)
Group S1, MS 606
Los Alamos, NM 87545
H. F. Martz
M. E. Johnson
R. A. Waller

Frank Abbey
United Kingdom Atomic Energy Authority
Safety & Reliability Directorate
Wigshaw Lane
Culcheth
Warrington WA3 4NE
UNITED KINGDOM

David C. Aldrich
SAIC
1710 Goodridge Drive
P.O. Box 1303
McLean, VA 22102

George Apostolakis
Mechanics and Structures Dept.
UCLA
Los Angeles, CA 90024

Nathaniel F. Barr
U.S. Department of Energy
Washington, DC 20545

Steve Bartell
Environmental Sciences Division
Oak Ridge National Laboratory
P.O. Box X
Oak Ridge, TN 37830

Paul Baybutt
Battelle Columbus Laboratories
505 King Avenue
Columbus, OH 43201

Anton Bayer
Kernforschnungszentrum Karlsruhe/INR
Postfach 3640
D-7500 Karlsruhe 1
WEST GERMANY

Thomas A. Bishop
Battelle Laboratories
505 King Avenue
Columbus, OH 43201

Klaus Burkart
Kernforschungszentrum Karlsruhe/INR
Postfach 3640
D-7500 Karlsruhe 1
WEST GERMANY

D. G. Cacuci
Oak Ridge National Laboratory
Engineering Physics Division
P.O. Box X
Oak Ridge, TN 37830

James E. Campbell
Intera Environmental Consultants Inc.
6850 Austin Center Blvd.
Suite 300
Austin, TX 78731

W. J. Conover
College of Business Administration
Texas Tech University
Lubbock, TX 79409

Michael Cullingford
P.O. Box 200
A-1400
Vienna
AUSTRIA

R. S. Denning
Battelle Columbus Laboratories
505 King Avenue
Columbus, OH 43201

Pamela Doctor
Battelle Northwest
P.O. Box 999
Richland, WA 99352

Darryl Downing
Computer Sciences
Building 2029, P.O. Box X
ORNL
Oak Ridge, TN 37830

Daniel Egan
Office of Radiation Programs (ANR-460)
U. S. Environmental Protection Agency
Washington, DC 20460

Joachim Ehrhardt
Kernforschungszentrum Karlsruhe/INR
Postfach 3640
D-7500 Karlsruhe 1
WEST GERMANY

Friedmar Fischer
Kernforschungszentrum Karlsruhe/INR
Postfach 3640
D-7500 Karlsruhe 1
WEST GERMANY

R. H. Gardner
Environmental Sciences Division
ORNL
Oak Ridge, TN 37830

F. M. Gelbard
17242 Walnut Street
Yorba Linda, CA 92686

Jim Gieseke
Battelle Laboratories
505 King Avenue
Columbus, OH 43201

William V. Harper
Performance Analysis Department
Battelle Laboratories
505 King Avenue
Columbus, OH 43201

Max Henrion
Dept. of Engineering and Public Policy
Carnegie-Mellon University
Pittsburgh, PA 15213

Edward Hofer
Gesellschaft für Reaktorsicherheit
D-8046 Garching
FEDERAL REPUBLIC OF GERMANY

F. O. Hoffman
Health and Safety Research Division
ORNL
Oak Ridge, TN 37830

Stephen C. Hora
Division of Business and Economics
University of Hawaii at Hilo
1400 Kapiolani St.
Hilo, HI 96720

Frank W. Horsch
Kernforschungszentrum Karlsruhe
Postfach 3640
D-7500 Karlsruhe 1
WEST GERMANY

H. Jordan
Battelle Laboratories
505 King Avenue
Columbus, OH 43201

Geoffrey D. Kaiser
Consulting Division
NUS Corporation
910 Clopper Road
Gaithersburg, MD 20878

G. Neale Kelly
NII/HSE
Silkhouse Court
Tithebarn Street
Liverpool L2 2LZ
UNITED KINGDOM

Klaus Kilpi
Technical Research Centre of Finland
Nuclear Engineering Laboratory
Loennratinkau 37
P.O. Box 169
SF-00181 Helsinki 18
FINLAND

Tom Kress
Bldg. 9108, MS-2
Oak Ridge National Laboratory
Oak Ridge, TN 37830

Greg McRae
Dept. of Chemical Engineering
Carnegie-Mellon University
Pittsburgh, PA 15213

M. Granger Morgan
Dept. of Engineering and Public Policy
Carnegie-Mellon University
Pittsburgh, PA 15213

E. M. Oblow
Oak Ridge National Laboratory
Engineering Physics Division
P.O. Box X
Oak Ridge, TN 37830

Derek J. Pike
Department of Statistics
The University of Reading
Whiteknights
Reading RG6 2AN
ENGLAND

Trevor Pratt
Brookhaven National Laboratory
Upton, NY 11973

Robert Ritzman
Electric Power Research Institute
3412 Hillview Avenue
Palo Alto, CA 94303

Ulf Tveten
Institute for Energy Technology
Postboks 40
N-2007 Kjeller
NORWAY

W. E. Vesely
Risk, Safety, and Reliability Section
Battelle Columbus Laboratories
505 King Avenue
Columbus, Ohio 43201

Eric R. Ziegel
Standard Oil Company (Indiana)
Amoco Research Center
P.O. Box 400
Naperville, IL 60566

2564 G. W. Smith
3141 S. A. Landenberger (5)
3151 W. L. Garner (1)
6312 M. S. Tierney
6400 A. W. Snyder
6410 J. W. Hickman
6412 M. P. Bohn
6415 D. J. Alpert
6415 J. M. Griesmeyer
6415 F. E. Haskin
6415 J. C. Helton (21)
6415 R. L. Iman
6415 J. D. Johnson
6415 C. D. Leigh
6415 M. J. Shortencarier
6415 J. L. Sprung
6422 J. E. Brockmann
6422 J. E. Gronager
6422 D. A. Powers
6431 R. M. Cranwell
6444 J. M. McGlaun
6444 S. W. Webb
6449 K. D. Bergeron
6449 K. K. Murata
6449 D. C. Williams
8024 P. W. Dean

NRC FORM 335 (2-84) NRCM 1102, 3201, 3202

U.S. NUCLEAR REGULATORY COMMISSION

BIBLIOGRAPHIC DATA SHEET

SEE INSTRUCTIONS ON THE REVERSE

1 REPORT NUMBER (Assigned by TIDC and Vol. No. if any)

NUREC/CR-4460
SAND85-2196

2 TITLE AND SUBTITLE

Uncertainty and Sensitivity Analysis of an Upper Plenum Test Problem for the MAEROS Aerosol Model

3 LEAVE BLANK

4 DATE REPORT COMPLETED

MONTH: December | YEAR: 1985

5 AUTHOR(S)

J. C. Helton, R. L. Iman, J. D. Johnson, C. D. Leigh

6 DATE REPORT ISSUED

MONTH: January | YEAR: 1986

7 PERFORMING ORGANIZATION NAME AND MAILING ADDRESS (Include Zip Code)

Sandia National Laboratories
P.O. Box 5800
Albuquerque, NM 87185

8 PROJECT/TASK/WORK UNIT NUMBER

9 FIN OR GRANT NUMBER

A-1339

10 SPONSORING ORGANIZATION NAME AND MAILING ADDRESS (Include Zip Code)

Division of Risk Analysis
Office of Nuclear Regulatory Research
U.S. Nuclear Regulatory Commission
Washington, DC 20555

11a TYPE OF REPORT

b PERIOD COVERED (Inclusive dates)

12 SUPPLEMENTARY NOTES

13 ABSTRACT (200 words or less)

The MAEROS aerosol model is being incorporated into the MELCOR code system for the calculation of risk from severe reactor accidents. To gain insight to assist in this incorporation, a computational test problem involving a three component aerosol in the upper plenum of a pressurized water reactor was analyzed with MAEROS. The following topics were investigated (1) the CRAY-1 CPU time requirements to implement and solve the system of differential equations on which MAEROS is based, (2) the effects on computational time and representational accuracy due to the use of different overall section boundaries and numbers of sections and components, and (3) the behavior of the aerosol and the variables which influence this behavior. Uncertainty and sensitivity analysis techniques based on Latin hypercube sampling and regression analysis were used in the investigation. Five sections and overall section boundaries from 0.1E-6 m to 50.E-6 m were found to be adequate for the problem under consideration. Further, solution time was found to be at least several hundred times faster than real time, which is felt to be adequate for MELCOR. Stepwise regression was used to investigate the sources of variation in computational time and suspended aerosol concentration.

14 DOCUMENT ANALYSIS - a KEYWORDS/DESCRIPTORS

b IDENTIFIERS/OPEN ENDED TERMS

15 AVAILABILITY STATEMENT

16 SECURITY CLASSIFICATION

(This page) Unclassified

(This report) Unclassified

17 NUMBER OF PAGES

18 PRICE